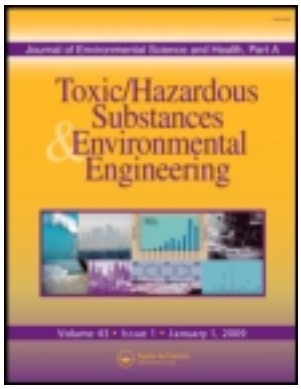

Journal of Environmental Science and Health, Part A: Toxic/Hazardous Substances and Environmental Engineering
Publication details, including instructions for authors and subscription information:
http://www.tandfonline.com/loi/lesa20

Measurements of respirable dust and nanoparticle concentrations in a titanium dioxide pigment production factory

Cheng-Hsiung Huang [a] , Chih-Yuan Tai [a] , Cheng-Yu Huang [b] , Chuen-Jinn Tsai [b] , Chun-Wan Chen [c] , Cheng-Ping Chang [c] & Tung-Sheng Shih [c]

[a] Department of Environmental Engineering and Health , Yuanpei University , Hsinchu, Taiwan

[b] Institute of Environmental Engineering, National Chiao Tung University , Hsinchu, Taiwan

[c] Institute of Occupational Safety and Health, Council of Labor Affairs , Executive Yuan, Taipei, Taiwan

Published online: 08 Jul 2010.

To cite this article: Cheng-Hsiung Huang , Chih-Yuan Tai , Cheng-Yu Huang , Chuen-Jinn Tsai , Chun-Wan Chen , Cheng-Ping Chang & Tung-Sheng Shih (2010) Measurements of respirable dust and nanoparticle concentrations in a titanium dioxide pigment production factory, Journal of Environmental Science and Health, Part A: Toxic/Hazardous Substances and Environmental Engineering, 45:10, 1227-1233, DOI: 10.1080/10934529.2010.493792

To link to this article: http://dx.doi.org/10.1080/10934529.2010.493792

Journal of Environmental Science and Health Part A (2010) **45**, 1227–1233

ISSN: 1093-4529 (Print); 1532-4117 (Online)
DOI: 10.1080/10934529.2010.493792

Taylor & Francis
Taylor & Francis Group

Measurements of respirable dust and nanoparticle concentrations in a titanium dioxide pigment production factory

CHENG-HSIUNG HUANG[1], CHIH-YUAN TAI[1], CHENG-YU HUANG[2], CHUEN-JINN TSAI[2], CHUN-WAN CHEN[3], CHENG-PING CHANG[3] and TUNG-SHENG SHIH[3]

[1] *Department of Environmental Engineering and Health, Yuanpei University, Hsinchu, Taiwan*
[2] *Institute of Environmental Engineering, National Chiao Tung University, Hsinchu, Taiwan*
[3] *Institute of Occupational Safety and Health, Council of Labor Affairs, Executive Yuan, Taipei, Taiwan*

This study compared respirable dust and nanoparticle concentrations measured by different sampling devices at a titanium dioxide pigment factory. Respirable particle mass concentrations, nanoparticle concentrations, particle size distribution and particle metallic content were measured at different sampling locations. The sampling results of the Multi-orifice Uniform Deposit Impactor (MOUDI) showed that the particle size distribution at this titanium dioxide production factory fell in the range of 1–10 μm. Generally, the higher levels of the respirable particle mass concentrations and nanoparticle number concentrations were near the packing site of the pigment titanium dioxide production factory. Metal analysis results revealed that the titanium dioxide concentrations in respirable dust and nanoparticles were within the limits specified by National Institute for Occupational Safety and Health (NIOSH). During sampling, particle metallic content analysis is essential for identifying the source of particles and for measuring respirable dust and nanoparticle concentrations.

Keywords: Respirable dust, nanoparticles, particle concentration, titanium dioxide.

Introduction

Titanium dioxide is widely found in consumer and industrial products. For instance, titanium dioxide is used in white pigments, coating materials, food colorants, sunscreens and cosmetic creams.[1–4] Worker exposure to titanium may occur during production and application processes such as packaging, grinding, cleaning and maintenance.[1,5,6] Garabrant et al.[7] indicated that 50% of all workers exposed to titanium dioxide suffered from respiratory symptoms and impaired pulmonary function. Epidemiological studies have demonstrated the relationship between the titanium dioxide particles in the air and increased morbidity from respiratory.[8–10] Ultrafine titanium dioxide particles (particle diameters smaller than 100 nm), or "nanoparticles", may cause inflammation, fibrosis, and impaired pulmonary function.[11–13] Ultrafine titanium dioxide particles might be able to enter the human stratum corneum and have the interaction with the immune system.[14,15] Studies showed that exposure to nano-sized titanium dioxide, even without UV irradiation, can cause proinflammatory effects in human endothelial cells.[16] Studies also confirmed that ultrafine particles may penetrate the respiratory tract more deeply compared to larger particles and that ultrafine particles can easily reach the alveoli region of the lung, where they interact with epithelial cells.[17–20]

Toxicological studies of male and female rats also indicated that 2 years of continuous exposure to 250 mg/m^3 pigmentary titanium dioxide particles increases the probability of pulmonary tumors, impairs particle clearance from the lung, and causes a persistent inflammatory response.[21,22] Compared to controls, inflammation and epithelial response is more evident in rats exposed to airborne pigmentary titanium dioxide.[23] Compared to fine particles (less than 2.5μm in diameter), ultrafine particles of titanium dioxide are more likely induce lung inflammation in rats.[24] Rat studies also indicated that lung overload with particulate material may cause tumorigenesis towards the

Address correspondence to Cheng-Hsiung Huang, Department of Environmental Engineering and Health, Yuanpei University, Hsin Chu, Taiwan; E-mail: chhuang@mail.ypu.edu.tw
Received December 17, 2009

end of the lifetime.[25] Therefore, after conducting in-depth research and probabilistic risk assessment of titanium dioxide toxicity, the United States National Institute for Occupational Safety and Health (NIOSH) suggested limits for occupational exposure to titanium dioxide (recommended exposure limit, REL).[26] The RELs for titanium dioxide fine particles and ultrafine particles are expressed in terms of time-weighted average concentration (time-weighted average concentration, TWA). The limits specified by NIOSH are 1.5 mg/m^3 for fine particles and 0.1 mg/m^3 for ultrafine particles.

A study regarding a titanium dioxide pigment production factory in the United States showed that workers were exposed to different levels of titanium dioxide.[27] Their results showed that packers, maintenance mechanics, and dry and wet treatment had the titanium dioxide measured levels of 6.2 ± 9.4 mg/m^3 (sample number, n=686), 2.5 ± 6.9 mg/m^3(n = 59), and 1.1 ± 1.1 mg/m^3(n = 117), respectively, with packers having the most exposure to titanium dioxide. Furthermore, studies also showed that workers exposed to titanium dioxide dust in yearly averaged estimated were 0.1–1.0 mg/m^3 for titanium dioxide pigment production factories in Europe. The mass concentrations of the individual occupational titles exposed to titanium dioxide dust were about 5 mg/m^3.[28] Few studies investigated the titanium dioxide concentration by analyzing the metallic content of the respirable dust and the nanoparticles in titanium dioxide pigment factories. It is thus important to conduct onsite measurement and metallic content analysis.

The main focus of this study is the concentration measurement of respirable particulate matter (RPM) and nanoparticles in a titanium dioxide pigment production factory. IOSH cyclone, MOUDI sampling device, and FMPS were used to measure the concentration of respirable particulate matter and nanoparticles, and to measure the particle size distribution. This work also compared the particle concentrations obtained by different sampling devices and analyzed the metallic content in particles.

Materials and methods

In this study, samples of respirable particulate matter and nanoparticles were obtained from a titanium dioxide pigment production factory for four times between April 2008 and February 2009. Figure 1 illustrates the sampling venue of the titanium dioxide pigment production factory. This study also investigated the particle size distribution and analyzed the metal content in particles at the titanium dioxide pigment factory. The sampling devices used is this study included a cyclone (IOSH cyclone, Institute of Occupational Safety and Health, Taiwan),[29] a Multi-orifice Uniform Deposit Impactor (MOUDI, Model 110, MSP Corp., St. Paul, USA), and a Fast Mobility Particle Sizer (FMPS, TSI Model 3091). The production process of the titanium

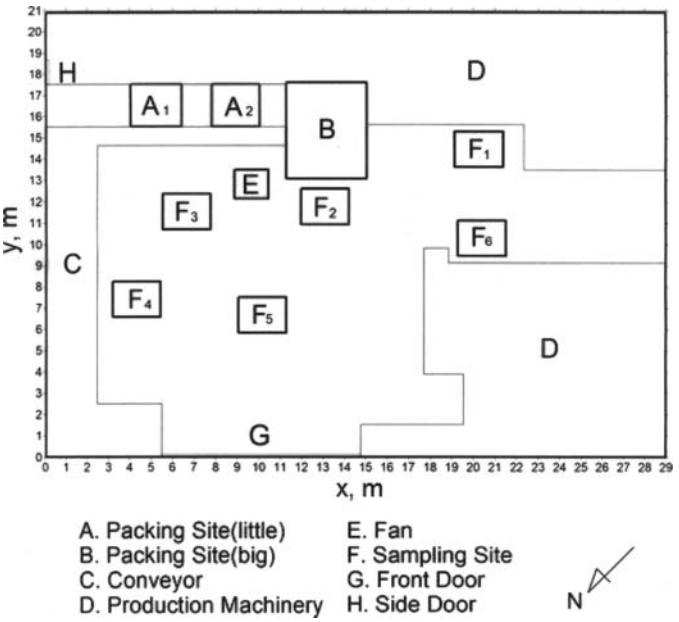

Fig. 1. Schematic diagram of titanium dioxide pigment factory.

dioxide pigment factory includes splitting and classifying titanium dioxide, removing the scattered salt particles from the substance, smashing the substance to obtain smaller particles, and transporting the titanium dioxide pigment to the pigment bagging area for packaging.

In the field sampling, two collocated IOSH cyclones used polytetrafluoroethylene (PTFE, SKC Inc., pore size of 2.0 μm and 37 mm) and mixed cellulose ester (MCE, SKC Inc., pore size of 0.8 μm and 37 mm) filters to obtain samples for weight measuring and metal concentration measuring, respectively; the flow rate was set at 1.7 L/min. The wind speeds at various sites were measured using a hot wire anemometer (Model:YK-2005AH, Pedak meettechniek, The Netherlands). When particles went into the IOSH cyclone, those over the size of 4 μm were collected by cyclone, while those less than 4 μm were collected by the bottom filter of the device. The concentration of the particles collected by polytetrafluoroethylene is equal to the weight concentration of respirable particulate matter. The samples collected by the mixed cellulose ester filter were then processed according to standard digestion procedures[30]; afterwards, they were analyzed for metal content using inductively coupled plasma - optical emission spectrometer (ICP-OES, OPTIMA 2100 DV, PerkinElmer, Shelton, CT, USA). In addition, the 0.056 μm filter and after filter of MOUDI, mixed cellulose ester filters, used ICP-OES to analyze the metal concentration of nanoparticles.

The containers used in the metal analysis were made of Polypropylene and Teflon. During the pre-treatment process, the containers were washed with mild detergent and immersed overnight in a solution made by 1 part nitric acid and 5 parts deionized water. The chemicals used were all specialized chemicals that are used for analyses produced

by the European company PANREAC Chemicals. The ion standard products used as the calibration and recovery were produced by Merck. The recoveries of metals varied between 94.2% and 103.1%. The detection limits of the apparatus were identified using a blank filter and were processed the same way as the samples. The Fe, Ti and Al detection limit of the IOSH cyclone for respirable particulate matter was 0.019, 0.0059 and 0.081μg/m^3, while the Fe, Mg, Ti and K detection limit of the MOUDI sampling device for nanoparticles was 0.0011, 0.0005, 0.0003 and 0.0031 μg/m^3, respectively.

The MOUDI sampling device used polytetrafluoroethylene and aluminum foil as filters for the particle size distribution measuring, and used mixed cellulose ester as filter for the metal concentration measuring. When the MOUDI sampling device is set at 30 L/min, it can obtain nominal cutoff aerodynamic diameters: 18, 10, 5.6, 3.2, 1.8, 1.0, 0.56, 0.32, 0.18, 0.10, 0.056 and <0.056 μm (after filter), respectively. After 24 hours of equilibration at 23 ± 3°C and relative humidity of 40 ± 5%, the MOUDI and IOSH cyclone samples used in the measuring process were pre- and post-weighed using a Microbalance (Mettler Toledo Inc, Switzerland). The weight concentration of particles collected by the MOUDI sampling device can be converted into the concentration of respirable particulate matter by the rate of respirable particle (*RF*) defined by the American Conference of Governmental Industrial Hygienists as the following equation.[31]

$$RF = (IF)\,(1 - F(x)) \tag{1}$$

$$IF(da, U_0) = 0.5\,(1 + \exp(-0.06da)) + 10^{-5}U_0^{2.75} \exp(0.055da) \tag{2}$$

$$F(\mathrm{x}) = 1 - 0.5(1 + 0.1969x + 0.1152x^2 + 0.0003x^3 + 0.0195x^4)^{-4} \quad \text{for} \quad x > 0 \tag{3}$$

$$F(\mathrm{x}) = 0.5(1 - 0.1969x + 0.1152x^2 - 0.0003x^3 + 0.0195x^4)^{-4} \quad \text{for} \quad x \le 0 \tag{4}$$

$$\mathrm{x} = 2.466 \ln(da) - 3.568 \tag{5}$$

where IF is the inhalable fraction; F(x) the cumulative fraction for a standardized normal variable x; *da* the cutoff aerodynamic diameter(μm); and U_0 is the air speed (m/s).

In this study, FMPS was mainly used to conduct mobile measurements. Six sampling points ($F_1 \sim F_6$) were established according to the locations of the interior and pigment bagging area of the titanium dioxide pigment factory. The main items measured included the number concentration of particles and their size distribution. The FMPS spectrometer accomplished particle size sorting based on differential electrical mobility classification. Particle concentration and size distribution can be obtained every second. Normalized particle number concentrations were then calculated in each channel according to the average concentration. The diameters of the particles measured by the FMPS were in the range of 5.6–560 nm.

Results and discussion

Particle size distribution

Figure 2 illustrates the particle size distribution obtained by the MOUDI sampling device at different time periods (Test I – Test IV) at sampling point F_3 of the titanium dioxide pigment factory. The mass median aerodynamic diameters (MMADs) of particles at sampling point F_3 observed in Tests I–IV were 5.52, 7.25, 4.79, and 6.0 μm, respectively; geometric standard deviations were 2.61, 2.84, 2.54, and 1.74, respectively. The sampling results showed that for each session, particle size was within the 1–10 μm range, and only a small proportion of particles at this work location were nanoparticles. The ratio of nanoparticle to submicron particle was 1.1% to 7.9%. The highest concentration of particles with diameters ranging from 1.0 to 1.8 μm was observed during Test I, probably because the fan was not operating during this test.

Respirable concentration comparison

Tests I–IV indicated that respirable dust concentrations obtained by the IOSH cyclone at sampling point F_3 of the titanium dioxide pigment factory were 487 μg/m^3, 688 μg/m^3, 268 μg/m^3, and 314 μg/m^3. Those obtained by MOUDI sampling device were 485 μg/m^3, 695 μg/m^3, 214 μg/m^3, and 321 μg/m^3. Figure 3 compares the concentrations obtained by the IOSH cyclone with those obtained by the MOUDI sampling device. The sampling devices obtained very similar respirable dust concentrations. Since the respirable dust concentration obtained by the IOSH cyclone approximated those obtained by the MOUDI sampling device, IOSH cyclones were used for further measurements of respirable dust mass concentrations at various stationary sampling points. The correlative equation for these two devices was Y=0.904X+51.7, and the R-squared was 0.988, which indicated a strong correlation between respirable dust concentration obtained by IOSH cyclone and that obtained by MOUDI sampling device.

Respirable concentrations at different locations

Table 1 shows the respirable dust mass concentrations obtained through the stationary sampling points F_1,

Table 1. Respirable dust concentrations of IOSH cyclone at various sampling points.

	Site F_1 μg/m^3	*Site* F_3 μg/m^3	*Site* F_4 μg/m^3	*Site* F_6 μg/m^3
Test I	335	487	375	295
Test II	195	688	587	233
Test III	80	268	224	80
Test IV	350	314	324	370

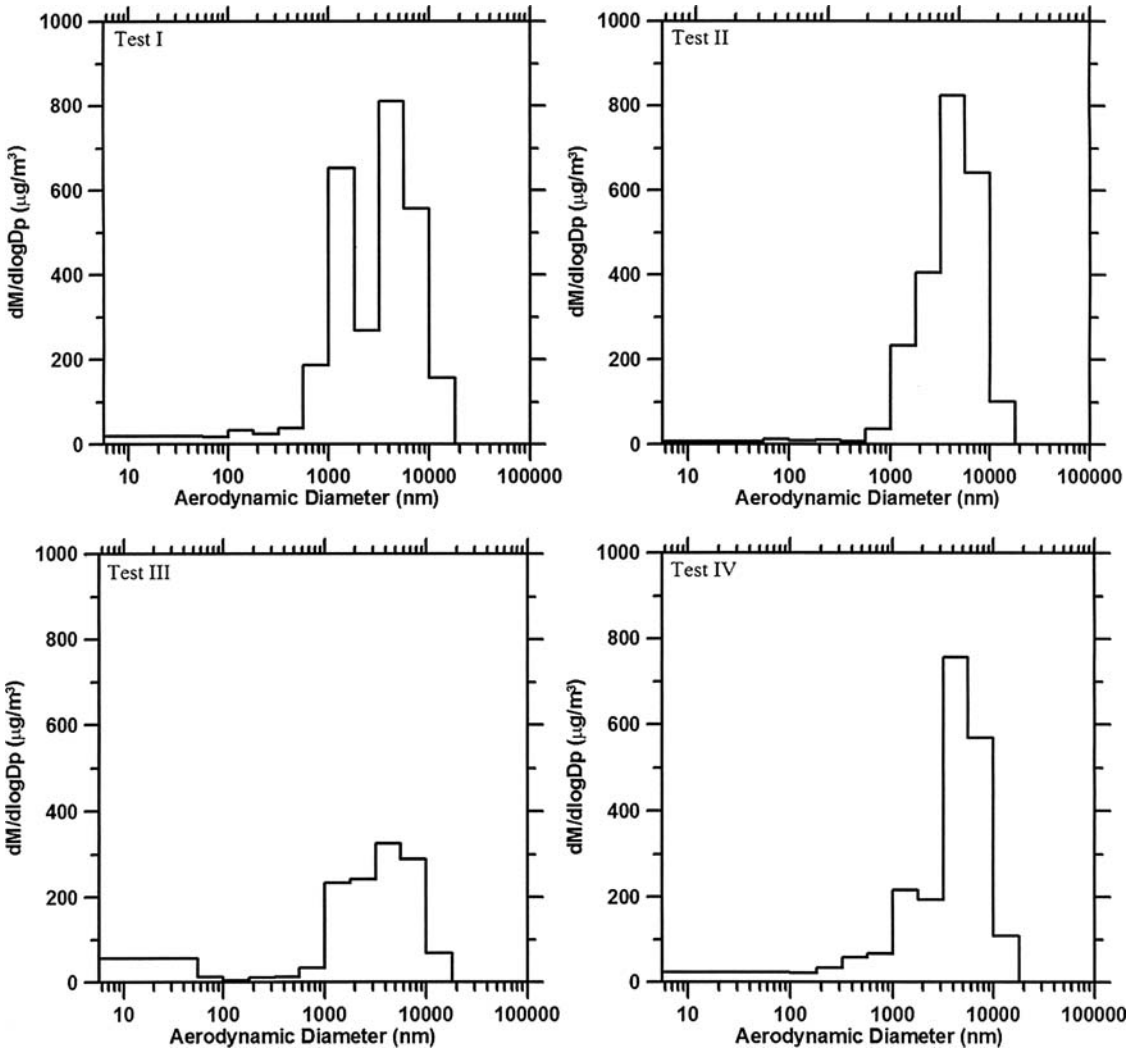

Fig. 2. Particle size distribution from MOUDI device at F_3 (Test I–Test IV).

F_3, F_4, and F_6. The results show that the concentration of the first measurement fell in the range of 295–487 $\mu g/m^3$; the second measurement fell in the range of 195–688 $\mu g/m^3$, the third measurement fell in the range of 80–268 $\mu g/m^3$, and the fourth measurement fell in the range of 314–370 $\mu g/m^3$. The concentration distribution shows that for the sampling points F_3 and F_4, the concentration of the second measurement was higher than that of the first measurement. Apparently, when the first measurements were made, the factory was packaging small 25-kilogram packages; when the second measurements were made, the factory was packaging large 800-kilogram packages. When packaging large amounts of titanium dioxide, a diesel fuel forklift moving from the front door towards the packing site was used to squeeze the air out of the wrapping. Such an action leads to a considerable amount of dust being released into the air. The forklifts also make several more trips than when processing small packages, leading to dust settling on the ground or on the packaging surfaces. For this reason, the second measurement had higher concentrations than the first measurement. Furthermore, the titanium dioxide pigment factory had natural ventilation and a floor-mounted fan was used during packaging process in the pigment bagging area. The wind speeds were about 0.3–1.4 m/s and the wind directions were from gate G towards the south in Test II. The concentration for sampling points F_3 and F_4 were higher because wind blowing from gate G resulting a stream circulation brought considerable amounts of respirable dust to sampling points F_3 and F_4. In the field, the wind speed measured at sampling site is less than 0.3 m/s, and the effect of wind speed on the measured respirable dust concentrations of the IOSH cyclones is negligible.[29]

The third measurement was conducted during the processing of small packages. The sampling results showed similar trends, but the concentrations were lower than that in the first measurement. The reason could be that the wind blowing from gate G was stronger and thus dispersed the

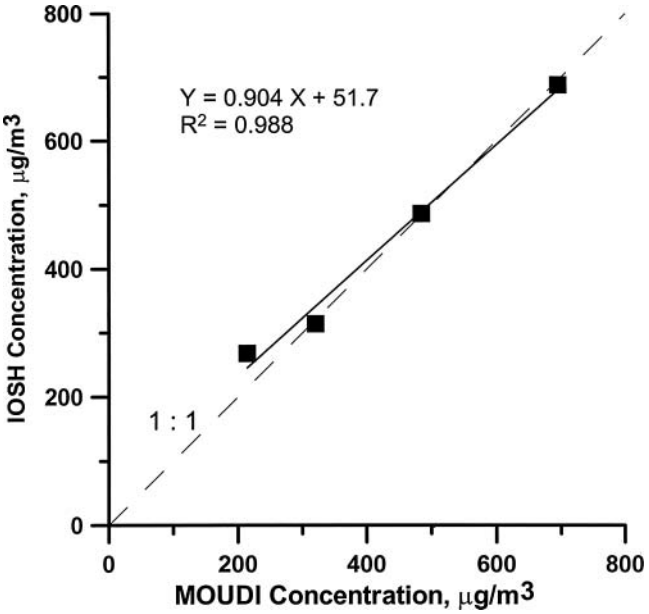

Fig. 3. Respirable dust concentration correlation between IOSH cyclone and MOUDI device at F_3 (Test I–Test IV).

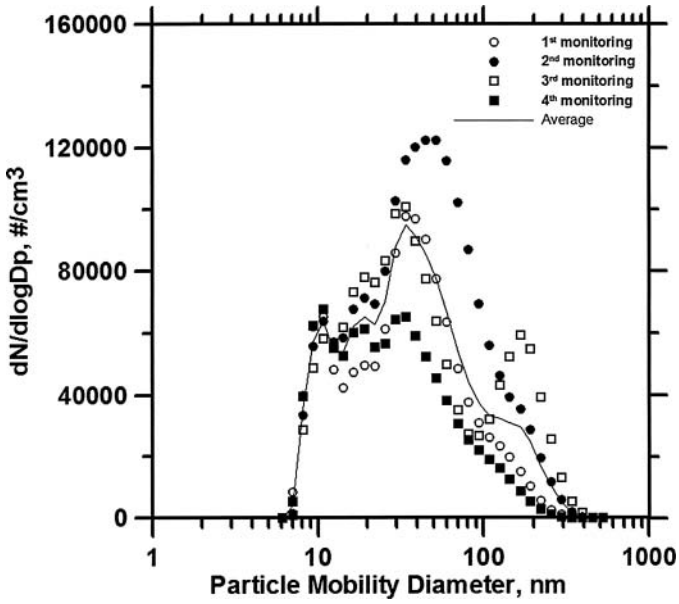

Fig. 4. Particle size distribution from FMPS measurements.

dust better. Additionally, the fan was turned on for a considerably longer time (205 minutes) during the third measurement than during the first measurement (100 minutes), leading to a lower concentration level during the third measurement. The fourth measurement is different to the other three measurements in that sampling points F_6 and F_1 had higher concentration levels. This could be due to the wind from gate G blowing towards a different direction. The wind was blowing towards the southeast (SE) from gate G during the third measurement, and towards the east (E) from gate G during the fourth measurement. This leads to a significant amount of respirable dust landing on sampling points F_1 and F_6, thus raising the concentration levels for the fourth measurement. In addition, the wind direction made it difficult for the respirable dust to exit from door H. Moreover, the fan was turned on for a considerably shorter period than that during the third measurement, leading to higher concentration levels.

Nanoparticle concentrations at different locations

In this study, mobile measurements were conducted at 6 measurement points (sites $F_1 \sim F_6$) for the first measurement in the pigment bagging area. Measurement results showed that the nanoparticle number concentration fell in the range of $4.9 \times 10^4 \sim 1.1 \times 10^5$ particles/cm^3. Figure 4 shows the particle size distribution as measured by FMPS at site F_3. The particle sizes mainly fell in the range of 10 nm to 80 nm, with the majority being close to 30-50 nm. The size distribution showed multiple peaks with one peak for most particles at the particle size of about 35 nm based on the average curve. Ultrafine particle emissions detected in the areas might be attributed to forklifts running or ambient atmosphere. It is worthwhile to investigate the attribution of ultrafine particles in the titanium dioxide pigment factory. Similar results can be found in the measurements of the bag filling activities of three plants.[32] Their results demonstrated that the forklift engine emitted ultrafine particles in the size range of 20–50 nm. Figure 5 shows the concentration map in the factory as measured through FMPS. The concentration distribution at the titanium dioxide pigment factory showed that the concentration levels at mobile points F_4, F_5, and F_6 were lower, and that higher concentration levels were found near points F_2 and F_3, especially near the packaging apparatus A_1. The concentration levels were elevated at A_1 probably because the wind blowing from gate G transported considerable amounts of nanoparticles.

Metal analysis

Table 2 shows the metal analysis results of the IOSH cyclone for Test I–Test IV. The metals detected at the pigment bagging area included titanium, aluminum, lead, iron, magnesium, and potassium. During the first measurement, three metals were identified (Fe, Ti, Al); the concentration levels were at their highest because the fan was not operating at this time, thus raising the titanium concentration levels at site F_3. Since the packaging process did not stop, some of the metals might have been generated through friction during the operation process. Test II–Test IV metal analyses results showed that Ti and Al were the main metal components. During these three sessions, the concentration levels of titanium were lower than Test I analysis. This is because

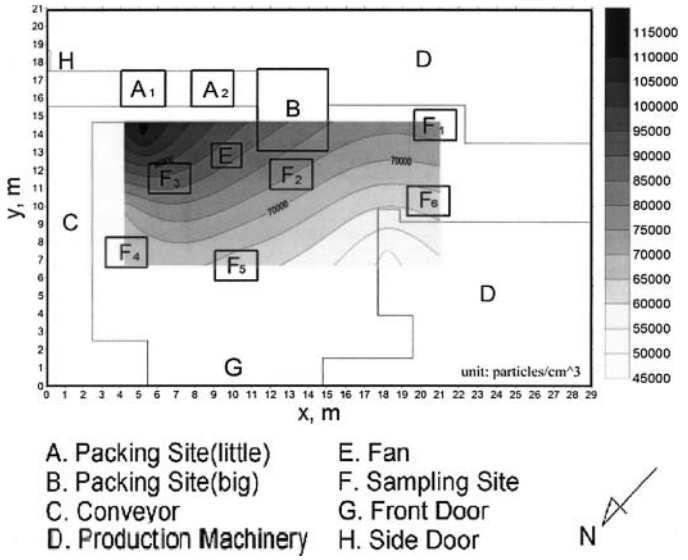

Fig. 5. Concentration map inside the factory according to FMPS measurements.

the fan was turned on and the titanium was blown away from the pigment bagging area for Tests II–IV.

In addition, the concentration levels of aluminum were not elevated relative to later tests due to titanium was the main component in the titanium dioxide pigment powder. However, the respirable dust concentration levels throughout the four sessions didn't differ as much. The reason is, during the four measurement sessions, the movement of the forklift and the workers raised the dust from the ground due to air turbulences, and the dust on the packaging also raised from its surface. In this study, titanium concentration was converted into titanium dioxide concentration, deriving 142.62 $\mu g/m^3$, 11.21 $\mu g/m^3$, 7.78 $\mu g/m^3$, and 5.99 $\mu g/m^3$ for Test I–Test IV, respectively. The values were within the 1500 $\mu g/m^3$limit for fine particles suggested by NIOSH.

Table 3 summarizes the metal analysis results of samples smaller than 100 nm obtained by the 0.056 μm-stage filter and after filter by the MOUDI sampling device at site F_3. Multiple analyses revealed that the nanoparticles detected during the four sessions were mainly Fe, Mg, Ti, and K. When converted into titanium dioxide concentration, the titanium dioxide mass concentrations of the nanoparticles detected in the study were 0.050 $\mu g/m^3$, N.D., 0.293 $\mu g/m^3$, and 0.176 $\mu g/m^3$. The values were within the 100 $\mu g/m^3$limit suggested by NIOSH. Thus, in this titanium dioxide pigment factory, the titanium dioxide mass concentration in the nanoparticles was expected to be low. The main metal components in the nanoparticles are slightly differed from those in the respirable particulate matter, possibly due to their different emission sources. Number concentrations of nanoparticles were detected at the titanium dioxide pigment factory and their values fell in the range of 4.9×10^4–1.1×10^5 particles/cm^3, possibly due to nanoparticles emitted from diesel forklift exhaust or nanoparticles in the outdoor environment. Generally, titanium dioxide concentrations in the respirable particulate matter and nanoparticles at this pigment factory were within the limits suggested by NIOSH. Additionally, the mass ratio of titanium dioxide concentrations in the nanoparticles to those in the respirable particulate matter ranged from 0.04% to 3.8%.

Table 2. Metal concentrations of IOSH Cyclone at F_3.

	Fe ($\mu g/m^3$)	*Ti* ($\mu g/m^3$)	*Al* ($\mu g/m^3$)
Test I	3.52	84.49	4.92
Test II	N.D.*	6.64	3.95
Test III	0.15	4.61	0.33
Test IV	N.D.	3.55	0.65

* N.D.: Not detectable.

Table 3. Metal concentrations of MOUDI device for nanoparticles.

	Fe ($\mu g/m^3$)	*Mg* ($\mu g/m^3$)	*Ti* ($\mu g/m^3$)	*K* ($\mu g/m^3$)
Test I	0.2446	N.D.*	0.0296	0.0063
Test II	N.D.	N.D.	N.D.	N.D.
Test III	0.1682	0.2302	0.1738	0.4805
Test IV	N.D.	0.0680	0.1043	N.D.

* N.D.: Not detectable.

Conclusions

Based on use of IOSH cyclone, MOUDI sampling device and FMPS, this study attempted to evaluate respirable dust and nanoparticle concentrations in a titanium dioxide pigment production factory. This work also measured particle distributions and particle metallic content. The sampling results indicated that the IOSH cyclone and the MOUDI sampling device obtained similar measurements of respirable dust concentrations. Particle metallic content analysis results showed that the titanium dioxide mass concentrations in respirable dust and nanoparticles were within the limits suggested by NIOSH. Meanwhile, the nanoparticle number concentration results showed that the most common particle size of the titanium dioxide pigments was 30–50 nm, and concentrations were of 4.9×10^4–1.1×10^5 particles/cm^3, possibly due to nanoparticles emitted from diesel forklift exhaust or blown into the workplace from outdoors. In addition, respirable dust concentration distributions were primarily subject to the impact of factors such as dust raised from diesel forklift movements, personnel movements and packaging surfaces, as well as external air entering the factory. Therefore, particle metallic content

analysis is essential to elucidating the source of the particles in the titanium dioxide pigment factory.

Acknowledgments

The authors would like to thank for the support of the Taiwan Institute of Occupational Safety and Health under the Contract number IOSH97-H104.

References

[1] Wang, J.J.; Sanderson, B.J.S.; Wang, H. Cyto- and genotoxicity of ultrafine TiO_2 particles in cultured human lymphoblastoid cells. Mutat. Res. **2007**, *628*, 99–06.

[2] Nordman, H.; Berlin, M. Titanium. In *Handbook on the Toxicology of Metals*; L. Friberg, G.F.; Nordberg; Vouk, V.B., Eds., Elsevier, Amsterdam, 1986.

[3] Lomer, M.C.; Thompson, R.P.; Powell, J.J. Fine and ultrafine particles of the diet: influence on the mucosal immune response and association with Crohn's disease. Proc. Nutr. Soc. **2002**, *61*, 123–130.

[4] Gelis, C.; Girard, S.; Mavon, A.; Delverdier, M.; Paillous, N.; Vicendo, P. Assessment of the skin photoprotective capacities of an organo-mineral broad-spectrum sunblock on two ex vivo skin models. Photodermatol. Photoimmunol. Photomed. **2003**, *19*, 242–253.

[5] Liao, C.-M.; Chiang, Y.-H.; Chio, C.-P. Assessing the airborne titanium dioxide nanoparticle-related exposure hazard at workplace. J. Hazard. Mater. **2009**, *162*, 57–65.

[6] Liao, C.-M.; Chiang, Y.-H.; Chio, C.-P. Model-based assessment for human inhalation exposure risk to airborne nano/fine titanium dioxide particles. Sci. Total Environ. **2008**, *407*, 165–177.

[7] Garabrant, D.H.; Fine, L.J.; Oliver, C.; Bernstein, L.; Peters, J.M. Abnormalities of pulmonary function and pleural disease among titanium metal production workers. Scand. J. Work Environ. Health **1987**, *13*, 47–51.

[8] Fayerweather, W.E.; Karns, M.E.; Gilby, P.G.; Chen, J.L. Epidemiologic study of lung cancer mortality in workers exposed to titanium tetrachloride. J. Occup. Environ. Med. **1992**, *34*, 164–169.

[9] Boffetta, P.; Gaborieau, V.; Nadon, L.; Parent, M.E.; Weiderpass, E.; Siemiatycki, J. Exposure to titanium dioxide and risk of lung cancer in a population-based study from Montreal Scand. J. Work Environ. Health **2001**, *27*, 227–232.

[10] Dharshana, K.G.T.; Coowanitwong, N. Ambient PM_{10} and respiratory illnesses in colombo city, Sri Lanka. Journal of Environmental Science and Health Part A,**2008**, *43*, 1064 – 1070.

[11] Baggs, R.B.; Ferin, J.; Oberdorster, G. Regression of pulmonary lesions produced by inhaled titanium dioxide in rats. Vet. Pathol.**1997**, *34*, 592–597.

[12] Rahman, Q.; Lohani, M.; Dopp, E.; Pemsel, H.; Jonas, L.; Weiss, D.G.; Schiffmann, D. Evidence that ultrafine titanium dioxide induces micronuclei and apoptosis in Syrian hamster embryo fibroblasts. Environ. Health Perspect. **2002**, *110*, 797–800.

[13] Kreilgaard, M. Influence of microemulsions on cutaneous drug delivery. Adv. Drug Deliv. Rev. **2002**, *54*, S77– S98.

[14] Lademann, J.; Weigmann, H.; Rickmeyer, C.; Barthelmes, H.; Schaefer, H.; Mueller, G.; Sterry, W. Penetration of titanium dioxide microparticles in a sunscreen formulation into the horny layer and the follicular orifice. Skin Pharmacol. Appl. Skin Physiol. **1999**, *12*, 247–256.

[15] Tinkle, S.S.; Antonini, J.M.; Rich, B.A.; Roberts, J.R.; Salmen, R.; DePree, K.; Adkins, E.J. Skin as a route of exposure and sensitization in chronic beryllium disease. Environ. Health Perspect. **2003**, *111*, 1202–1208.

[16] Peters, K.; Unger, R.E.; Kirkpatrick, C.J.; Gatti, A.M.; Monari, E. Effects of nano-scaled particles on endothelial cell function in vitro: studies on viability, proliferation and inflammation. J. Mater. Sci. Mater. Med. **2004**, *15*, 321–325.

[17] Nel, A. Air pollution-related illness: effects of particles. Science **2005**, *306*, 804-806.

[18] Peters, A.; Wichmann, H.E.; Tuch, T.; Heinrich, J.; Heyder, J. Respiratory effects are associated with the number of ultrafine particles. Am. J. Respir. Crit. Care Med. **1997**, *155*, 1376–1383.

[19] Jaques, P.A.; Chong, S.K. Measurement of total lung deposition of inhaled ultrafine particles in healthy men and women. Inhal. Toxicol. **2000**, *12*, 715–731.

[20] Brown, J.S.; Zeman, K.L.; Bennett, W.D. Ultrafine particle deposition and clearance in the healthy and obstructed lung. Am. J. Resp. Crit. Care Med. **2002**, *166*, 1240–1247.

[21] Lee, K.P.; Trochimowicz, H.J.; Reinhardt, C.F. Pulmonary response of rats exposed to titanium dioxide (TiO_2) by inhalation for two years. Toxicol. Appl. Pharmacol. **1985**, *79*, 179–192.

[22] Cullen, R.T.; Tran, C.L.; Buchanan, D.; Davis, J.M.; Searl, A.; Jones, A.D.; Donaldson, K. Inhalation of poorly soluble particles. I. Differences in inflammatory response and clearance during exposure. Inhal. Toxicol. **2000**, *12*, 1089–1111.

[23] Bermudez, E.; Mangum, J.B.; Asgharian, B.; Wong, B.A.; Reverdy, E.E.; Janszen, D.B.; Hext, P.M.; Warheit, D.B.; Everitt, J.I. Long-term pulmonary responses of three laboratory rodent species to subchronic inhalation of pigmentary titanium dioxide particles. Toxicol. Sci. **2002**, *70*, 86–97.

[24] Ferin, J., Oberdorster, G.; Penney, D.P. Pulmonary retention of ultrafine and fine particles in rats. Am. J. Respir. Cell Mol. Biol. **1992**, *6*, 535–542.

[25] Hext, P.M. Current perspectives on particulate induced pulmonary tumours. Human Exp. Toxicol. **1994**, *13*, 700–715.

[26] National Institute for Occupational Safety and Health (NIOSH). *NIOSH current intelligence bulletin: evaluation of health hazard and recommendations for occupational exposure to titanium dioxide*, DHHS (NIOSH) publication. Cincinnati, Ohio, 2005.

[27] Fryzek, J.P.; Chadda, B.; Marano, D.; White, K.; Schweitzer, S.; McLaughlin, J.K. A cohort mortality study among titanium dioxide manufacturing workers in the United States. J. Occup. Environ. Med. **2003**, *45*, 400–409.

[28] Boffetta, P.; Soutar, A.; Cherrie, J.W.; Granath, F.; Andersen, A.; Anttila, A. Mortality among workers employed in the titanium dioxide production industry in Europe. Cancer Causes Control. **2004**, *15*, 697–706.

[29] Tsai, C.-J.; Shiau, H.-G.; Shih, T.-S. Field study of the accuracy of two respirable sampling cyclones. Aerosol Sci. Technol. **1999**, *31*, 463–472.

[30] National Institute for Occupational Safety and Health (NIOSH). *Elements by ICP: Method 7300, Issue 2,* NIOSH Manual of Analytical Methods (NMAM), Fourth Edition,1994.

[31] Hinds, W.C. *Aerosol technology*; John Wiley and Sons, New York, 1999.

[32] Kuhlbusch, T.A.J.; Neumann, S.; Fissan, H. Number Size Distribution, Mass concentration, and particle composition of PM_1, $PM_{2.5}$, and PM_{10} in bag filling areas of carbon black production. J. Occup. Environ. Hyg. **2004**, *1*, 660–671.